Investigation of Induction Heating in Asphalt Mortar: Numerical Approach

Apostolidis, Panos; Liu, X.; Scarpas, Athanasios; van de Ven, Martin; van Bochove, G

Publication date
2016

Document Version
Accepted author manuscript

Published in
Investigation of Induction Heating in Asphalt Mortar: Numerical Approach

Investigation of Induction Heating in Asphalt Mortar: Numerical Approach

P. Apostolidis[1], X. Liu[1], T. Scarpas[1], M.F.C. van de Ven[1] and G. van Bochove[2]

[1] Section of Pavement Engineering
Faculty of Civil Engineering and Geosciences, Delft University of Technology
Stevinweg 1, 2628 CN Delft, the Netherlands
Tel. +31 61 6599128, Email: p.apostolidis@tudelft.nl

[2] Heijmans, Heijmans Integrale Projecten B.V.
Graafsebaan 3, 5248 JR Rosmalen, the Netherlands
Tel. +31 73 5435425, Email:gbochove@heijmans.nl

Corresponding author:
P. Apostolidis
E-mail: p.apostolidis@tudelft.nl

Total Number of Words

Words in abstract	=	141	words
Words in text:	=	4085	words
Words in references	=	517	words
Figures: (11x250)	=	2750	words equivalent
Total	=	7493	words equivalent

Submitted for publication and presentation for the 95th meeting of the Transportation Research Board, January 10-14, 2016

ABSTRACT

The research reported in this paper focuses on utilization of advanced finite-element analyses (COMSOL) for the design and assessment of the induction heating capacity of asphalt mortar by adding electrically conductive additives (e.g., steel fibers), and to understand the factors that influence the mechanisms of induction heating in asphalt mixtures. In order to determine numerically the effective electrical and thermal properties of the conductive asphalt mortar with different volumes of steel fibers, 3D finite element meshes were generated by using X-ray images and utilized for calibration of the model parameters to perform a more realistic simulation of the asphalt mixture induction healing. The findings of this research are part of a study to provide an optimization method for the development of the necessary tools and equipment that will enable the implementation of induction technology for healing of asphalt concrete mixtures.

INTRODUCTION

Asphalt mixtures are widely used in the construction industry mainly for the transportation infrastructure and are considered to be self healing materials. Because of its natural ability to recover mechanical properties, such as strength and stiffness, asphalt mixes autonomously heal during hot summers and long rest periods (*1*-*4*). This self healing capacity of asphalt mixes has a large impact on the service life of the asphalt pavements. If a fast healing process can be initiated at the right time, the lifetime of the asphalt concrete mixtures can significantly be prolonged. In this case the life cycle cost can be reduced and also the traffic disruptions due to maintenance activities can be minimized.

Induction heating techniques have been applied widely in the metallurgical and semiconductor industry for bonding, hardening or softening of metals or conductive materials (*5*-*7*). Recently, efforts were made to develop innovative techniques to accelerate the healing capability of asphalt mixes, see Figure 1, (*8*-*12*). It has been shown that the induction heating of asphalt mixtures can significantly improve the mechanical performance of asphalt mixes by healing of the micro-cracks and preventing the formation of macro-cracks.

However, more data is still required to clarify the role and the significance of the various parameters on the asphalt heating phenomenon. Particularly, induction heating is a complex phenomenon that combines the electromagnetic and heat transfer theory, and has a strong relationship with the electro-magneto-thermal properties of materials (*13*-*15*). The necessity of experimental and numerical analysis of electro-magneto-thermo-mechanical properties of asphalt mixtures is becoming very important in terms to determine the most crucial material parameters for obtaining enhanced durability, simultaneously with high induction heating rate.

It is well known that asphalt concrete mixtures are characterized as non-conductive materials, but when conductive additives are mixed into the asphalt mixtures, they become suitable for induction heating. The asphalt mixtures can be heated locally under a time-variable magnetic. Specifically, when an alternating electric current is applied to an induction coil, a time-variable magnetic field is generated on this. According to Faraday's law, this magnetic field induces currents (eddy currents) in the additives within the mixture, such as steel fibers, and they are heated up based on the principles of the Joule law, see Figure 1.c. The generated heat in the additives increases locally the temperature of the asphalt mortar rather than heating the stone aggregates, through the temperature rise the bitumen is melting, the micro-cracks are healed and the mechanical properties are recovered. This mechanism is known as induction healing of asphalt mixtures.

As previously described, additives are required into the asphalt mixtures in order to make them suitable for induction heating. Addition of electrically conductive fibers is much more effective than to add conductive filler-sized particles (*9*) and also the volume of these and bitumen influences the induction heating efficiency (*11*). It was also observed that the thermal and the electrical conductivity as well as the induction heating efficiency are dependent of the volume of steel fibers in asphalt mixtures (*12*). Consequently, apart from the operational conditions – frequency, intensity of the magnetic field, etc - the efficiency of this type of electromagnetic heating is dependent on the effective properties of the asphalt mixtures with steel fibers and other additives.

It is obvious that although there has been conducted experimental studies in order to evaluate the impact of conductive additives on induction heating efficiency, still limited research was issued to quantify the influence of different operational parameters of an induction system on heating efficiency of asphalt mixes. The present paper, which studies the important factors of induction heating in asphalt mixes, presents the theoretical background of phenomena behind the induction heating technique. Asphalt mortar - asphalt mix without the stone fraction - is selected to be studied here because it is the part of asphalt concrete where conductive fibers are dispersed notably, contributing to the final mechanical performance and electro-thermal properties of asphalt (*16, 17*). The 3D finite element meshes of asphalt mortars with different volumes of steel fibers are generated using X-ray scans in order to evaluate the effective electrical and thermal properties.

After the numerical determination of important induction parameters for the conductive asphalt mortar, a finite element 3D model of electromagnetic phenomena coupled with heat transfer physics is developed. The current FE model provides us this efficient tool to conduct analysis of induction heating predicting in parallel the heating time needed in order to heal micro-cracks inside of asphalt mixes. It should be taken into account that the recommended surface temperature of asphalt mortar to obtain sufficient healing recovery is 85 ^{o}C (*11*).

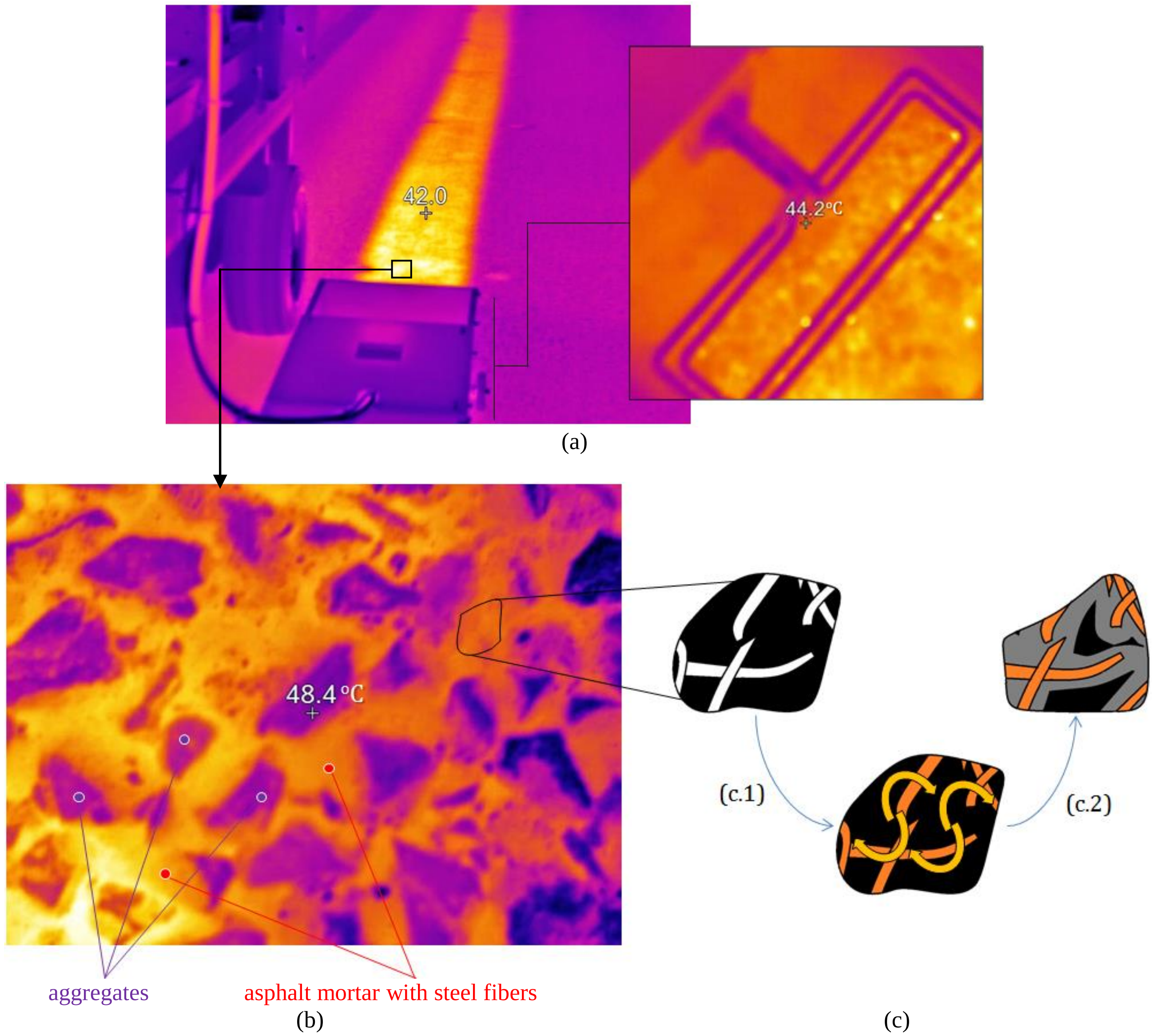

FIGURE 1 Infrared image (a) during induction heating of an asphalt pavement (A58 near Vlissingen, the Netherlands), (b) of heated asphalt pavement surface at high resolution and (c) the schematic of induction heating of asphalt mortar with steel fibers (c.1) induced by eddy currents and (c.2) heat generation in the mortar based on the Joule's law

THEORETICAL BACKGROUND

Fundamentals of Electromagnetic Field Phenomena

Maxwell's equations describe the electromagnetic field phenomena by involving four different field variables: the electric flux density vector **D** [C/m^2] or [As/m^2], the magnetic flux density vector **B** [A/m], the electric field intensity vector **E** [V/m] and the magnetic field intensity vector **H** [A/m^2], and are given in the following equations 1, 2, 3 and 4:

$$\nabla \times \mathbf{E} = -\frac{\partial \mathbf{B}}{\partial t} \tag{1}$$

which is known as Faraday's law and describes that the induced currents in the asphalt mixture with conductive additives have the same frequency, but the opposite direction as the supplied electric current by the induction coil.

$$\nabla \times \mathbf{H} = \mathbf{J} + \frac{\partial \mathbf{D}}{\partial t} \tag{2}$$

which is known as Ampere's law in which **J** is the current density. The equation (2) describes that the applied alternating electric current on induction coil will produce in its surrounding area an alternating magnetic field with the same frequency as the induction coil current.

$$\nabla \cdot \mathbf{D} = \rho \tag{3}$$

which is known as Gauss's electric field law and ρ is the free volume charge density [C/m^3] or [As/m^3].

$$\nabla \cdot \mathbf{B} = 0 \tag{4}$$

which is known as Gauss's magnetic field law.

To include the main constitutive equations of electromagnetic phenomena, the following demonstrates the relationship between the electric flux and the intensity of the field

$$\mathbf{D} = \varepsilon_0 \cdot \varepsilon_r \cdot \mathbf{E} = \varepsilon \cdot \mathbf{E} \tag{5}$$

wherein ε is the electric permittivity ([F/m] or [As/m]) of the asphalt mixture with conductive additives. The permittivity is the product of the electric permittivity of vacuum ε_0 ($8.854 \cdot 10^{-12}$ As/Vm) and the relative electric permittivity (ε_r). The last one describes the ability of a material to conduct the electric field better than vacuum or air and it is one for conductive materials.

The relation between the magnetic flux and field intensity is

$$\mathbf{B} = \mu_0 \cdot \mu_r \cdot \mathbf{H} = \mu \cdot \mathbf{H} \tag{6}$$

where μ is the permeability [H/m] or [Vs/A]. The permeability of vacuum is constant with a value $\mu_0 = 4\pi \cdot 10^{-7}$ Vs/Am. The relative magnetic permeability μ_r describes the ability of a material to conduct the magnetic flux better than a vacuum or air and has a remarkable impact on all basic induction heating phenomena, coil calculation and computation of electromagnetic field distribution.

Concerning the association of current density with the electric field density, the continuum form of Ohm's law is expressed as

$$\mathbf{J} = \sigma \cdot \mathbf{E} \tag{7}$$

in which σ is the electrical conductivity [S/m] or [A/Vm].

The Maxwell equations represent a system of coupled first-order differential equations and they can be reduced to two second-order equations. Then, the magnetic flux **B** can be expressed by a vector potential **A** as:

$$\mathbf{B} = \nabla \times \mathbf{A} \tag{8}$$

wherein **A** is the magnetic vector potential.

Based on the Faraday law from Maxwell's equations

$$\nabla \times \mathbf{E} = -\frac{\partial \mathbf{B}}{\partial t} = -\frac{\partial}{\partial t}(\nabla \times \mathbf{A}) = -\nabla \times \frac{\partial \mathbf{A}}{\partial t} \tag{9}$$

Due to the fact that

$$\nabla \times \left(\mathbf{E} + \frac{\partial \mathbf{A}}{\partial t}\right) = \nabla \times (\nabla \varphi) = 0 \tag{10}$$

then,

$$\mathbf{E} = -\frac{\partial \mathbf{A}}{\partial t} - \nabla \varphi \tag{11}$$

Multiplication of the electric field with the electrical conductivity σ gives

$$\mathbf{J} = \sigma \mathbf{E} = -\sigma \frac{\partial \mathbf{A}}{\partial t} - \sigma \nabla \varphi = -\sigma \frac{\partial \mathbf{A}}{\partial t} + \mathbf{J_s} \tag{12}$$

in which **Js** is the source current density in the induction coil.

Assuming that the simplification of divergence of a curl is zero and the displacement current is negligible in a material with high electrical conductivity

$$\nabla \times \mathbf{H} = \mathbf{J} \tag{13}$$

Results in

$$\nabla \times \frac{1}{\mu}\mathbf{B} = \mathbf{J} \tag{14}$$

Substituting equations, the diffusion equation is

$$\sigma \frac{\partial \mathbf{A}}{\partial t} - \frac{1}{\mu}\nabla^2 \mathbf{A} = \mathbf{J_s} \tag{15}$$

In the case of working with the sinusoidal current excitation, and the sinusoidal eddy current as well, a time-harmonic electromagnetic field is introduced

$$i\omega\sigma\mathbf{A} - \frac{1}{\mu}\nabla^2 \mathbf{A} = \mathbf{J_s} \tag{16}$$

In the electrically conductive asphalt mixture is an induced current density denoted by J_{eddy}. The equation for the asphalt mixture is

$$i\omega\sigma\mathbf{A} - \frac{1}{\mu}\nabla^2 \mathbf{A} = 0 \tag{17}$$

where

$$-i\omega\sigma\mathbf{A} = \mathrm{J_{eddy}} \tag{18}$$

Fundamentals of Heat Transfer Phenomena

Heat transfer occurs in three different modes, conduction, convection and radiation. With regards to the heat conduction mode, the constitutive equation of the Fourier law is given by

$$q_{cond} = -k\nabla T \tag{19}$$

where k is the thermal conductivity tensor of the asphalt mixture [W/(m^{o}C)], T is the temperature [^{o}C] and q_{cond} is the heat flux by conduction.

The heat convection from the surface of the mixture to the ambient fluid or gas can be defined by the following equation 20

$$q_{conv} = h(T_s - T_\infty)^a \quad (20)$$

where h is the convection surface heat transfer coefficient [W/(m^{2o}C)], T_s is the surface temperature [^{o}C], T_∞ is the ambient temperature [^{o}C] and q_{conv} is the heat flux density by convection [W/m^2].

Moreover, heat losses transferred from the hot conductive asphalt mixture due to the electromagnetic radiation is known as thermal radiation and is described by equation 21

$$q_{rad} = sigma \cdot em[(T_s)^4 - (T_\infty)^4] \quad (21)$$

where sigma is the Stefan-Boltzmann constant (sigma=$5.67 \cdot 10^{-8} W/m^2K^4$) and em is the emissivity of the surface.

Induction Heating Coupling Equations

A finite element model predefined in the COMSOL Multiphysics software (*19*, *20*), which can simulate electro-magnetic and thermo-mechanical phenomena in a real time system, has been utilized for modelling of the induction heating in the conductive asphalt mortar. The electromagnetic field is modeled by means of the magnetic field intensity vector **A** [A/m^2] and the magnetic flux density vector **B** [A/m] as shown in equation 22

$$(j\omega\sigma - \omega^2 \varepsilon_0 \varepsilon_r)\mathbf{A} + \nabla \times \left(\frac{1}{\mu_0 \mu_r}\mathbf{B}\right) - \sigma \mathbf{v} \times \mathbf{B} = J_\varphi{}^e \quad (22)$$

where J denotes the imaginary unit and ω the angular frequency of the harmonic current.

The model was created by using a Single-Turn Coil domain feature and the governing equation of the induction coil under frequency-transient study analysis is given by:

$$I_{coil} = \int_{\partial\Omega} \mathbf{J} \cdot \mathbf{n} \quad (23)$$

where I_{coil} denotes the flowing current of the coil.

Finally, the heating equation governed by the Fourier heat transfer equation is defined by:

$$\rho c_p \frac{\partial T}{\partial t} + \rho c_p \mathbf{u} \cdot \nabla T = \nabla \cdot (k \nabla T) + Q \quad (24)$$

where ρ is the density, c_p is the specific heat capacity, k is the thermal conductivity and Q is the energy generated in the asphalt mixture per unit volume and time.

NUMERICAL DETERMINATION OF ELECTRO-THERMAL PROPERTIES OF ASPHALT MORTAR

Previous researches (*9*, *12*) indicated that, by adding electrically conductive additives (e.g., steel fibers), an asphalt mixture can be heated up in a very short time by using the induction heating technology. In order to simulate the effective electrical and thermal properties of conductive asphalt mixtures, the 3D finite element meshes of conductive asphalt mortars - as a representative of the asphalt mixtures without stone aggregates - with different volumes of steel fibers are generated by using High-resolution X-ray CT (Computed Tomography) images.

The High-resolution X-ray CT is a completely nondestructive technique for visualizing features in the interior of opaque solid objects, and for obtaining digital information on their 3-D geometries and properties. By the X-ray CT technology, the different densities of individual components (e.g., sand, filler, air voids and bitumen) in the asphalt mortar can be distinguished by the gray levels in a CT slice.

SIMPLEWARE software was utilized to comprehensively process 3D image data and to generate volume and surface meshes from the image data (*18*). Meshes can be directly imported into the COMSOL Multiphysics finite-element software for the electrical and thermal conductivity analyses. The process of reconstruction of 3D images of conductive asphalt mortars is illustrated in Figure 2.a. The 3D images of the asphalt mortar with different steel fibers contents are presented in Figure 2.b.

For the determination of electro-thermal properties of the conductive asphalt mortar, it is necessary to predefine the properties of individual components in the asphalt mortar. Therefore, in this investigation, the magnitudes of the electrical and thermal conductivity of the bitumen, mineral filler and sand were assumed to be 9e-5 S/m and 0.487 W/(m·K) respectively and for steel fiber 20e+3 S/m and 16 W/(m·k) were assumed. The effective electrical and thermal conductivities of the conductive asphalt mortar with different volume fractions of fiber are determined numerically and given in Figure 3.

The results in Figure 3 indicate that the electrical conductivity of the asphalt mortar increased with increasing the content of steel fiber. As it can be noticed, the electrical conductivity of the asphalt mortar increases rapidly when the volume fraction of the steel fiber is close to 6%. The reason of this dramatic increase of the electrical conductivity can be explained by the percolation threshold theory. The percolation threshold is reached when the shorter conductive pathways are formed by the higher amount of steel fibers in the asphalt mortar. Similarly, it can be observed that, with the stepwise increase of steel fibers in the asphalt mortar, the effective thermal conductivity of the conductive asphalt mortar is increased from 0.71 W/(m·K) to 1.58 W/(m·K). This happened because the thermal conductivity of steel fibers is higher than the other components in the asphalt mortar.

According to the current numerical analysis, the improvement of effective electrical and thermal conductivity is dependent on the proportion of steel fibers in the asphalt mortar. Moreover, it is well known that it is difficult to obtain experimentally precise conductivity results from asphalt mixtures (*16*). Therefore, this method of numerical analysis of asphalt mortar properties could be proved effective tool to determine the electro-thermal characteristics of conductive asphalt mixes. Subsequently, understanding the conductivity mechanism is also the other advantage of this numerical technique where the transformation phenomenon of asphalt mix, from insulator to conductor, can be quantified by identifying the percolation threshold limit.

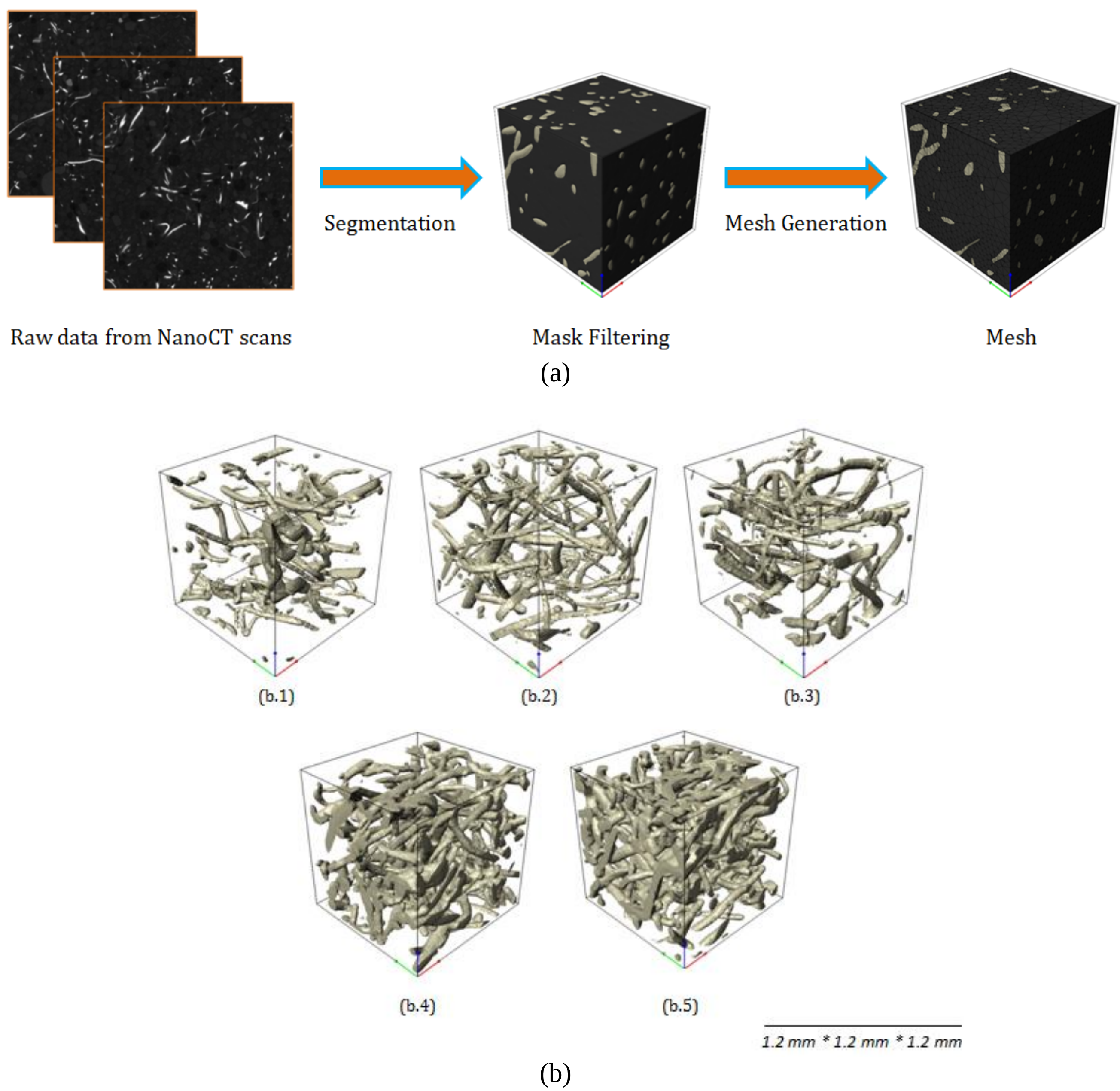

FIGURE 2 (a) Overview of 3D image data post processing and (b) reconstructed images after segmenting the NanoCT-scans for the conductive asphalt mortars with different steel fibers content; (b.1) 3.4 %, (b.2) 4.7 %, (b.3) 5.2 %, (b.4) 6.8 % and (b.5) 13.3 % of steel fibers

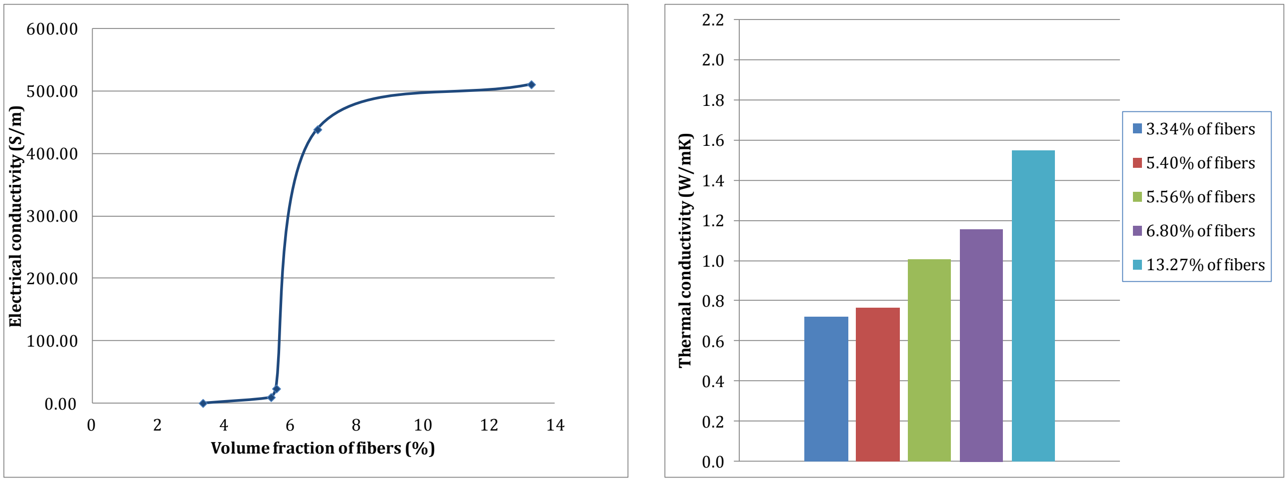

(a) (b)

FIGURE 3 Numerically determined effective (a) electrical and (b) thermal conductivity of different asphalt mortars

FINITE ELEMENT MODELS AND PARAMETERS

In order to study the influence of frequency, power and distance of coils on the induction heating capacity of the conductive asphalt mortar, two finite element (FE) models were utilized. One model makes use of one induction coil at a distance of 50 mm above the surface of the mortar sample, Figure 4.a.1. In the second model, an additional coil is used at a distance of 200 mm above the surface of the mortar, Figure 4.a.2. The induction coils with a square cross-section of side 0.1 m were assumed. By imposing the alternative current to the coils, eddy current can be generated in the vicinity of the conductive asphalt mortar. It should be noted that the geometry of the induction coil has significant impact on the induction heating efficiency (*5*, *6*). For this reason, the higher order tetrahedral elements were utilized to model the coils and the entire induction heating system, see Figure 4.b.1 & b.2. In addition to the coils, each model consists of one layer of the conductive asphalt mortar with a thickness of 30 cm, one layer of ground sand soil underneath the mortar layer and air above the mortar layer.

Normally the electrical-thermal properties of conductive asphalt mixtures are temperature dependent. However, for simplicity, the electro-thermal properties of the conductive asphalt mortar are assumed constant in the simulations.

In order to make the asphalt mortar conductive, it was assumed that 6% of steel fibers was added into the asphalt mixture. The electrical and thermal conductivity of the conductive asphalt mortar were taken from the numerical analysis from the previous section. Furthermore, in the following numerical simulations, the parameters of the relative permeability and heat capacity of the conductive mortar were assumed to be 1 and 920 J/(kg·K) respectively. Moreover, an ambient temperature of 20 ^{o}C was assumed to simulate the induction heating operation at normal environmental conditions. The duration of the induction heating in the simulation was 120 second. The applied power voltage and the frequency of the alternating magnetic field were set to 550 V and 64 kHz for the simulations based on previous experimental experience (*12*).

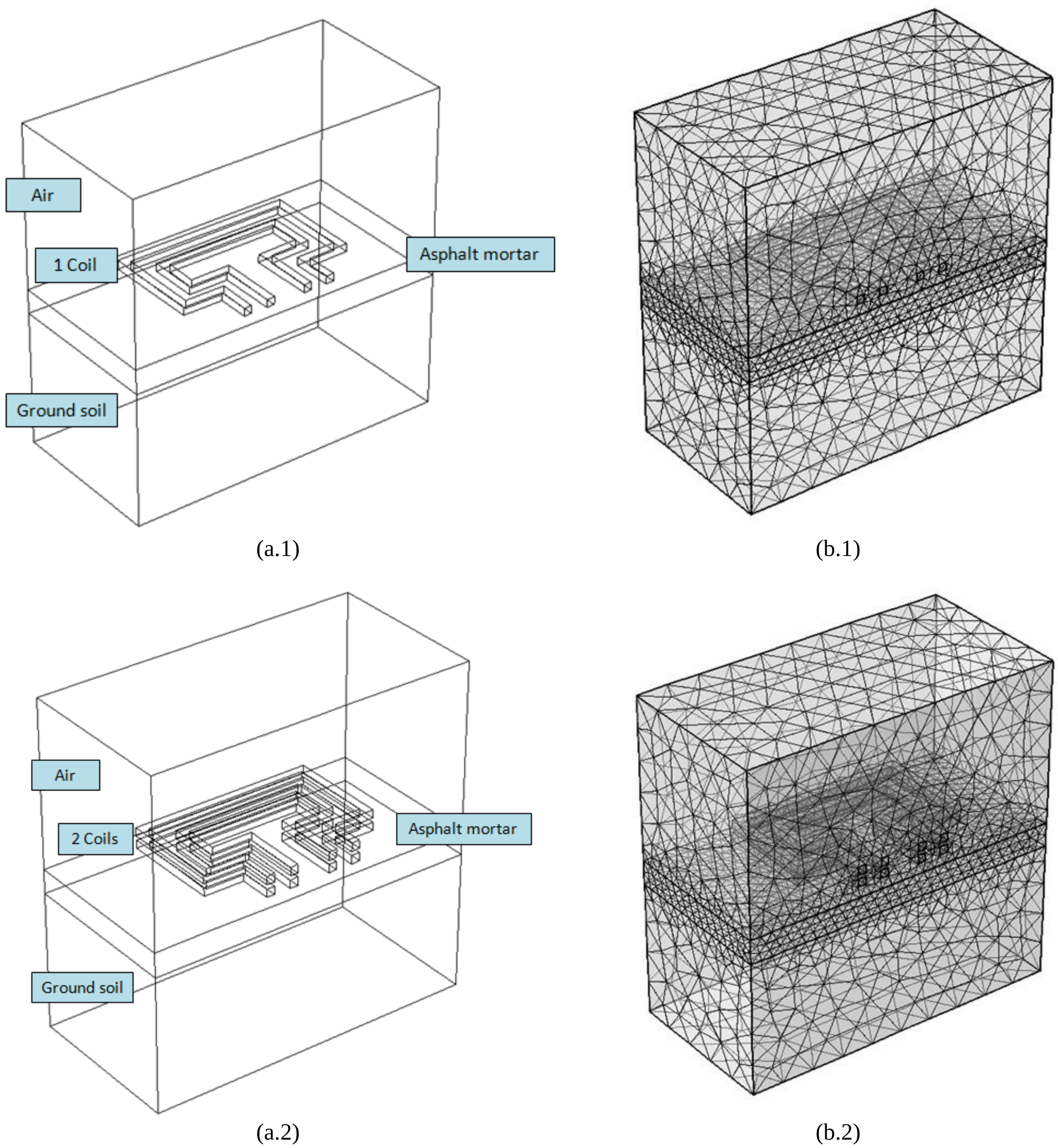

FIGURE 4 Schematic of (a.1) one coil and (a.2) two coils induction systems at 3D; and the relative mesh refinements (b.1 and b.2)

RESULTS AND DISCUSSION

Effect of Electrical and Thermal Properties

The numerical simulations for the one coil system were carried out first. The distribution of magnetic flux density and temperature on the conductive asphalt mortar are shown in Figure 5. The influence of the electrical conductivity on the temperature distribution within the cross-section of the asphalt mortars is shown in Figure 6. It should be noted that the asphalt mortar with 100 S/m of electrical conductivity corresponds to the response of the asphalt mortar mixed with 6% of steel fibers. Hence, the asphalt mortar with 1 S/m of electrical conductivity represents the mortar mixed with a very low amount of steel fibers.

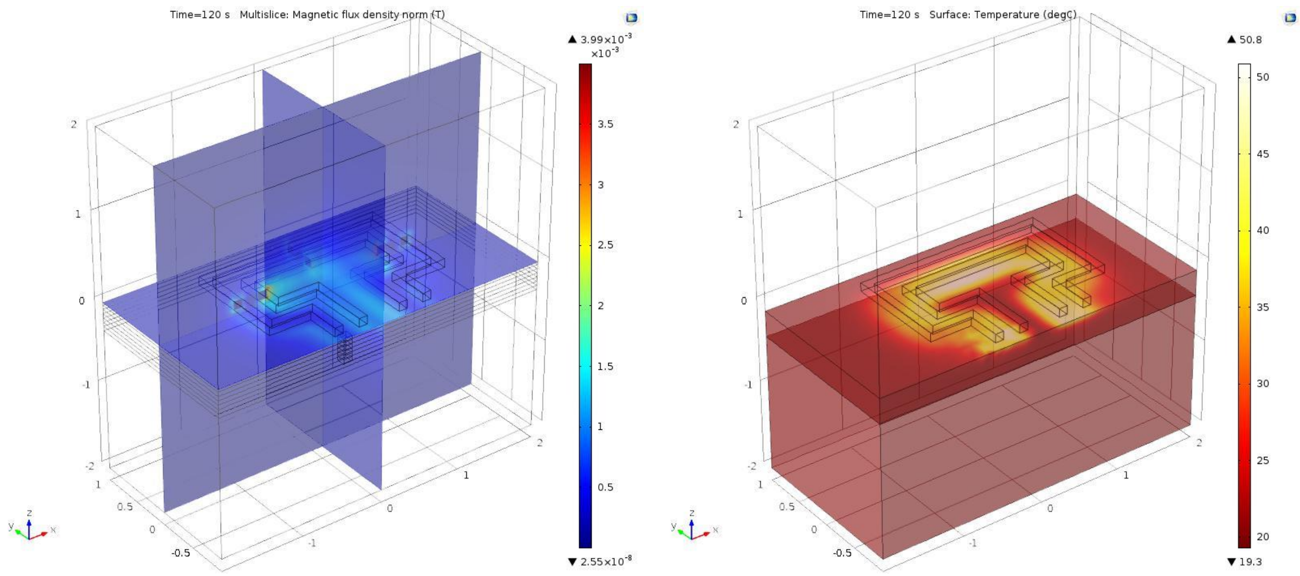

(a) (b)

FIGURE 5 (a) Magnetic flux density and (b) temperature distribution at the end of induction heating

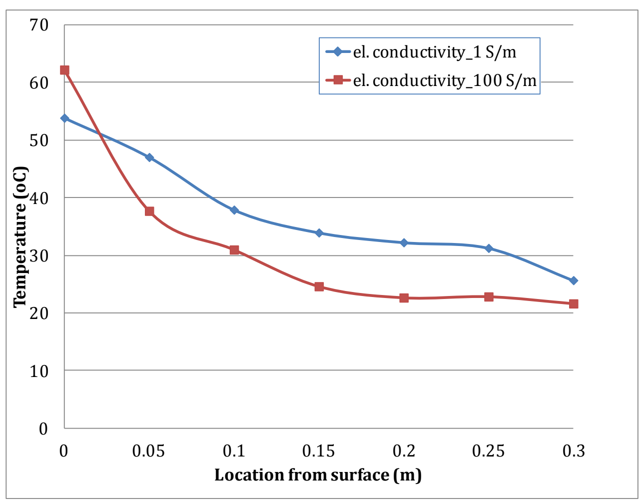

FIGURE 6 Influence of the electrical conductivity of the conductive asphalt mortars on temperature distribution (induction time 120s, one induction coil system)

It can be observed in Figure 6 that, after 120 seconds of induction heating, for the case of the asphalt mortar with 100 S/m of electrical conductivity, the surface temperature is higher than with 1 S/m (lower amount of steel fibers). This finding supports the observations made by previous researches (*12*), where the induction heating efficiency appears to be proportional to the volume of the conductive additives added in the asphalt mixes.

The amount of steel fibers can also influence the thermal gradient inside the asphalt mortar, see Figure 6. For example, for the case of asphalt mortar with 100 S/m of electrical conductivity, the temperature decreases faster inside the mortar, than the case 1 S/m. This thermal gradient difference is caused by the skin effect. When a conductive asphalt mortar has a high electrical conductivity, the alternating magnetic field induces electric currents which are concentrated on the surface of the conductive asphalt mortar. The high concentration of the electric currents leads to a higher heat generation at the surface of the conductive asphalt mortar. Therefore the asphalt mortar with higher electrical conductivity (e.g., 100 S/m) has a higher temperature at the surface but a lower temperature inside the material.

In Figure 7, the effect of thermal conductivity and heat capacity of conductive asphalt mortars is also presented. The parametric analyses are done for conductive asphalt mortar with two different heat capacities (e.g., 875 and 925 J/(kg·K)), four different thermal conductivities(e.g., 0.5, 0.7, 0.9, 1.1 W/(m·K)), while the electrical conductivity of the compared mortars is constant (100 S/m). By comparing to Figure 6, it can be concluded that the impact of the thermal properties of the asphalt mortar on the temperature distribution is not of the same importance with the effect of electrical conductivity.

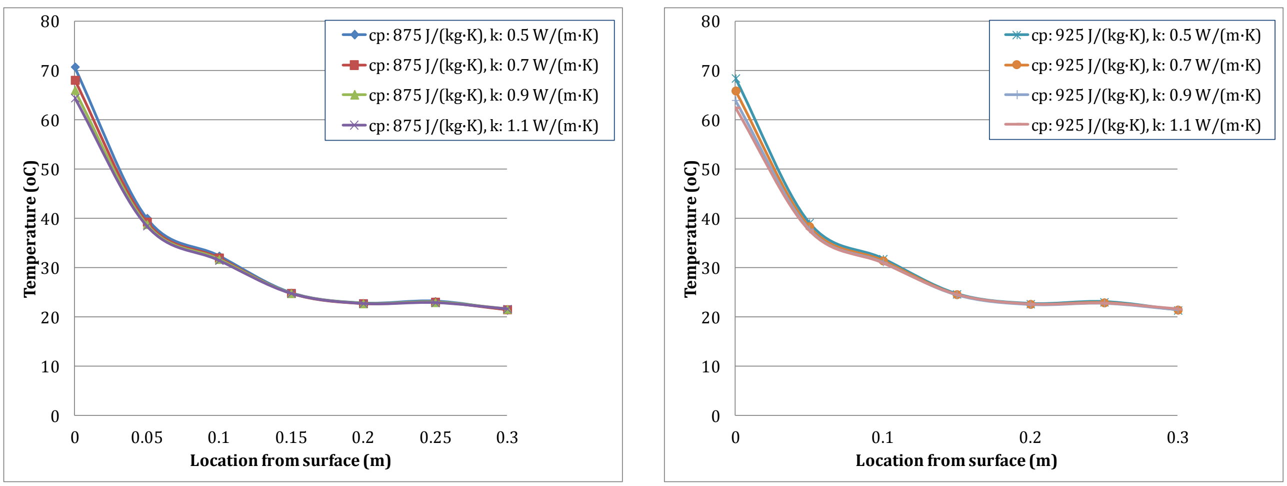

(a) (b)

FIGURE 7 Influence of the thermal conductivity and heat capacity of the conductive asphalt mortars on temperature distribution (electrical conductivity 100 S/m, induction time 120s, one induction coil system)

Effect of Operational Parameters

The numerical results in Figure 8 show that the distance between the induction coil and the conductive mortar can influence significantly the heat generation in the conductive asphalt mortar. By increasing the coil distance from 50 mm to 100 mm to the mortar surface, it leads to 50% reduction of the temperature at the surface of the asphalt mortar. This means that for surface induction heating coil closer to the surface is more efficient one at larger distance from the surface of the asphalt mortar. Moreover, the tendency is similar for the materials with different electrical conductivity values.

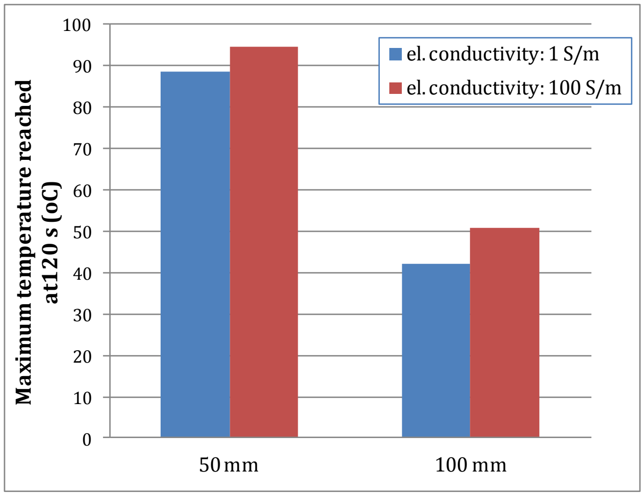

FIGURE 8 Maximum temperature generated by the single coil system at the different electrical conductivities at the different coil distances to the conductive asphalt mortar (one induction coil system)

The power and the frequency of the alternating magnetic field of the induction machine are two important operational parameters that can influence significantly the induction heating efficiency of the conductive asphalt mortar. Figure 9 shows the comparison of the effect of the power and the frequency of the induction coil on the temperature distribution inside the conductive asphalt mortar. It can be observed that, at the same frequency (e.g., 30 kHz), higher machine power results in higher temperatures generated in the material over the whole height.

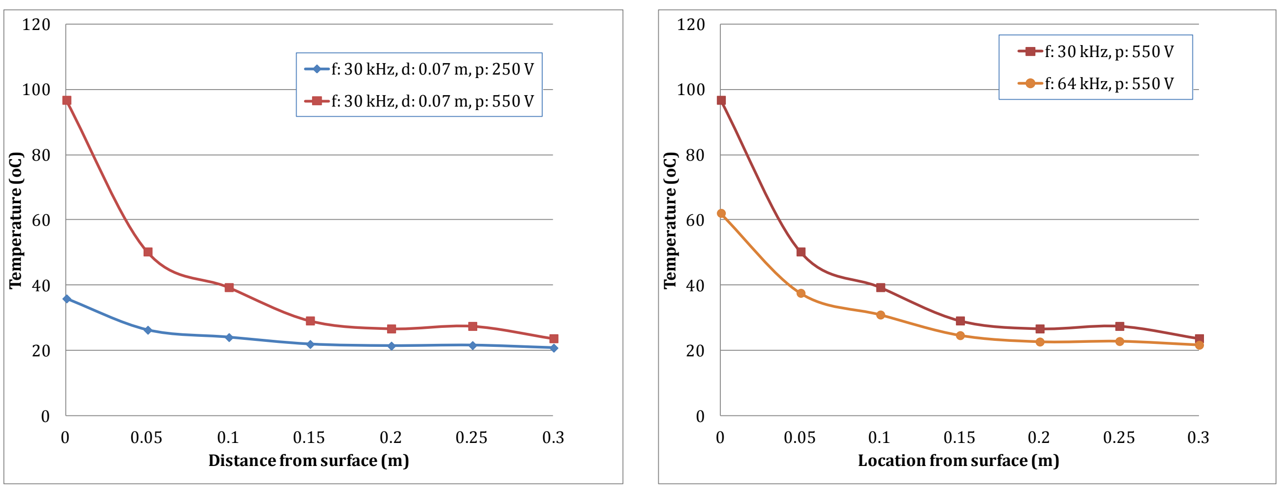

(a) (b)

FIGURE 9 Influence of (a) the supplied power and (b) the frequency of induction coil (electrical conductivity 100 S/m, induction time 120s, one induction coil system)

On the other hand, the frequency of the magnetic field is another important operation parameter. It can be seen that, at constant voltage (e.g., 550 V), the lower frequency of 30 kHz leads to higher maximum surface temperature than the higher frequency of 64 kHz. The distributions of the temperature within the cross-section of the conductive asphalt mortar show the same tendency for the both cases.

Effect of Two Coils Induction System

In order to show the possibilities for guidance for the induction machine design, the influence of two coils system on the heating efficiency of the asphalt mortar was also studied. The influence of the supplied powers of the two induction coils system and the distance of the upper induction coil to the sample surface is presented.

Figure 10.a shows the plots of the temperature distribution in the asphalt mortar with 6% of steel fibers for the different combinations of the power of the bottom and the top induction coil. It can be observed that the power of the coil closer to the surface of the induction material has a significant effect on the heat generation. When the power of both coils is doubled from 250 V to 500 V, the induction heating efficiency of the system increases by 8%. The distributions of the temperature within the cross-section of the conductive asphalt mortar show the same tendency for both cases.

With the bottom coil at constant distance (50 mm) to the sample surface, the induction heating efficiency decreases with increasing the distance of the top coil, see Figure 10.b. Increase of the distance of the top coil to the sample surface from 180 mm to 280 mm, leads to reduction of the heat efficiency. Despite the fact that the maximum temperature drops because of the increase of the distance of the top coil to the sample surface, the distribution of the temperature within the cross-section of the conductive asphalt mortar show the same tendency for all the cases.

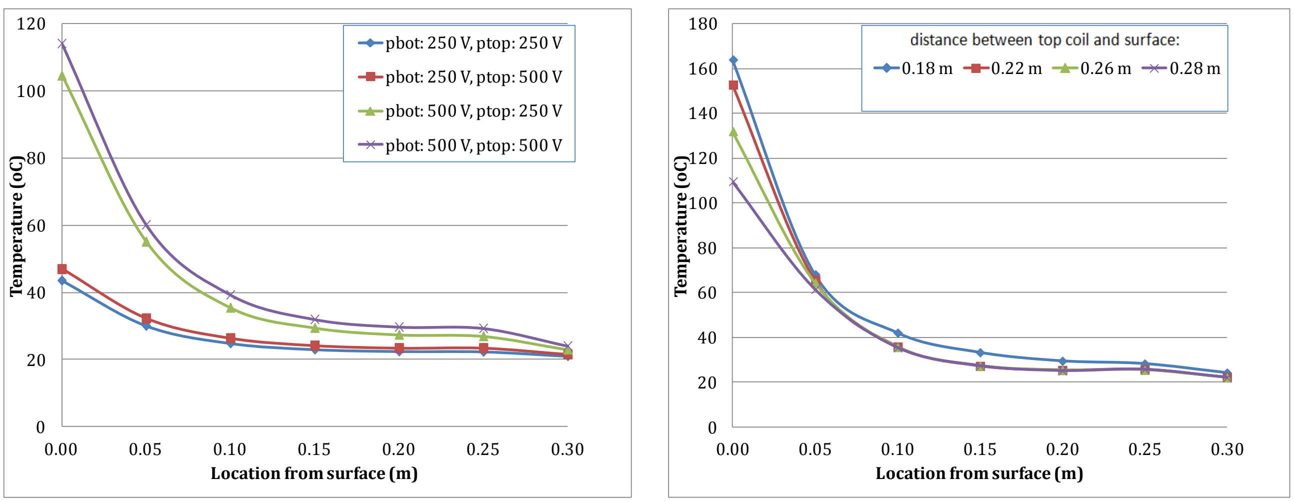

(a) (b)

FIGURE 10 Influence of (a) the supplied powers of the two induction coils system (frequency 64.5 kHz, electrical conductivity 100 S/m, induction time 120s) and (b) the distance of the upper induction coil to the sample surface (frequency 64 kHz, electrical conductivity 100 S/m, induction time 120s)

Finally, a comparison of the two coils system with the one coil system is presented in Figure 11. It can be observed that, at the same induction time (120 s), the two coils induction system generates two times higher surface temperature the one coil induction system. Also, the two coil induction system is more powerful and efficient for asphalt concrete healing application, because it can generate higher temperatures in the top part of the first layer which enables the contractor to heal the micro cracks quickly at this place. Thus, the induction heating technique can be approved very highly efficient for preserving pavement surface defects, such as the raveling, when two coils systems are utilized.

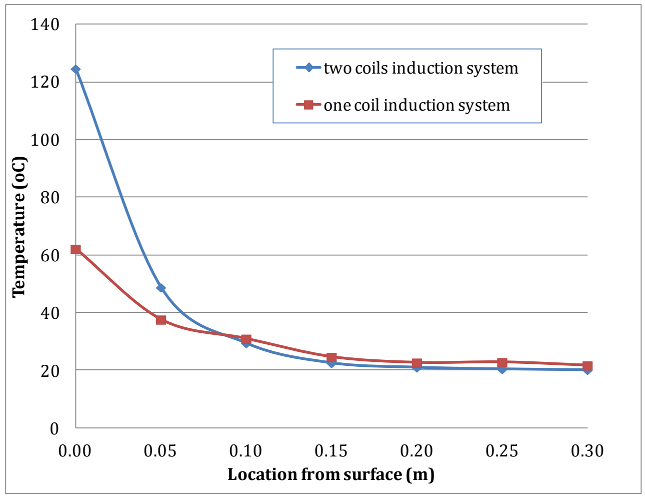

FIGURE 11 Comparison of the different types of induction coil systems on heating distribution in the conductive asphalt mortar (electrical conductivity 100 S/m, induction time 120s)

CONCLUSIONS

The electrical and thermal characteristics of a conductive asphalt mortar play important role for the design and assessment of the induction heating capacity of asphalt concrete mixtures. The application of FEM to evaluate the effective properties of conductive asphalt mixes and the different operational conditions of induction heating is proved to be a very effective tool, capable to perform analysis without conducting time consuming and costly experiments. The 3D induction heating FE model enables us to calibrate the model parameters to perform more realistic heating simulations for asphalt concrete mixtures. Lastly, the valuable findings of this research show that it is possible to optimize the necessary tools and equipment needed for the implementation of the induction technology for heating and subsequently healing asphalt pavements.

REFERENCES

1. Little, D.N., A. Bhasin. Exploring mechanisms of healing in asphalt mixtures and quantifying its impact. In *Self Healing Materials: An Alternative Approach to 20 Centuries of Materials Science* (S. van de Zwaag, ed.) Springer Series in Materials Science, Vol. 100, Springer, Dordrecht, the Netherlands, 2007, pp. 205-218.
2. Qiu, L. *Self healing of asphalt mixtures. towards a better understanding of the mechanism*. Ph.D. Dissertation, Delft University, 2012.
3. Williams, D., D.N. Little, R.L. Lytton, Y.R. Kim, Y. Kim. *Microdamage healing in asphalt and asphalt concrete.* Research report 7229, A&M University, College Station, 2001.
4. Kim, B., R. Roque. Evaluation of healing property of asphalt mixtures. In *Transportation Research Record: Journal of the Transportation Research Board, No. 1970*, Transportation Research Board of the National Academies, Washington, D.C., 2006, pp. 84-91.
5. Ahmed, T.J., D. Stavrov, H.E.N. Bersee, A. Beukers. Induction welding of thermoplastic composites - an overview. *Composite Part A.: Applied Science and Manufacturing*, Vol. 37, 2006, pp. 1638-1651.

6. Rapoport, E., Y. Pleshivtseva. *Optimal control of induction heating processes*. Taylor and Francis Group, 2007.
7. Rudolf, R., P. Mitschang, M. Neitzel. Induction heating of continuous carbon-fibre reinforced thermoplastics. *Composite: Part A*, Vol. 31, 2000, pp. 1191-1202.
8. Garcia, A., E. Schlangen, M. van de Ven. Two ways of closing cracks on asphalt concrete pavement: microcapsules and induction heating. *Key Engineering Materials*, Vol. 417-418, 2010, pp 573-576.
9. Garcia, A., E. Schlangen, M. van de Ven, Q. Liu. Electrical conductivity of asphalt mortar containing conductive fibers and fillers. *Construction and Building Materials*, Vol. 23, 2009. pp. 3175-3181.
10. Liu, Q., W. Yu, E. Schlangen, G. van Bochove. Unravelling porous asphalt concrete with induction heating. *Construction and Building Materials*, Vol. 71, 2014, pp. 152-157.
11. Liu, G., E. Schlangen, M. van de Ven. Induction healing of porous asphalt concrete. *In Transportation Research Record,: Journal of the Transportation Research Board*, *No 2305,* Transportation Research Board of the National Academies, Washington, D.C., 2012, pp. 95-101.
12. Garcia. A., J. Norambuena-Contreras, M.N. Partl. Experimental evaluation of dense asphalt concrete properties for induction heating purposes. *Construction and Building Materials*, 46, 2013, pp. 48-54.
13. Mesquita, R.C., J.P.A. Bastos. 3D finite element solution of induction heating problems with efficient time-stepping. *IEEE Transactions of Magnetics*, Vol. 27, No. 5, 1991, pp. 4065-4068.
14. Boadi, A., Y. Tsuchida, T. Todaka, M. Enokizono. Designing of suitable construction of high-frequency induction heating coil by using finite-element method. *IEEE Transactions on Magnetics*. Vol. 41, No. 10, 2005, pp. 4048-4050.
15. Wang, Z., W. Huang, W. Jia, Q. Zhao, Y. Wang, W. Yan. 3D Multifields FEM computation of transverse flux induction heating for moving-strips. *IEEE Transactions on Magnetics*. Vol. 35, No. 3, 1999, pp. 1642-1645.
16. Wu, S., P. Pan, F. Xiao. Conductive asphalt concrete: A review on structure design, performance and practical applications. *Journal of Intelligent Material Systems and Structures*. 2013.
17. Anderson, D.A., T.W. Kennedy. Development of SHRP binder specification. *Journal of the Association of Asphalt Paving Technologists*. 62, 1993, pp. 481-507.
18. *Simpleware*. ScanIP, +ScanFE, 2011.
19. *COMSOL. AC/DC Module* – User's Guide. Version 4.4. 2013.
20. *COMSOL. Heat Transfer Module* – User's Guide. Version 4.4. 2013.